Journal of Power Sources 188 (2009) 427–432

Contents lists available at ScienceDirect

Journal of Power Sources

journal homepage: www.elsevier.com/locate/jpowsour

Improvement of methanol electro-oxidation activity of PtRu/C and PtNiCr/C catalysts by anodic treatment

Min Ku Jeon, Paul J. McGinn*

Department of Chemical and Biomolecular Eng., University of Notre Dame, 178 Fitzpatrick, Notre Dame, IN 46556, USA

ARTICLE INFO

Article history:
Received 17 November 2008
Accepted 26 November 2008
Available online 3 December 2008

Keywords:
Methanol electro-oxidation
Direct methanol fuel cell
Anodic treatment
Cyclic voltammetry
Chronoamperometry

ABSTRACT

The effect of an anodic treatment on the methanol oxidation activity of PtRu/C (50:50 at.%) and PtNiCr/C (Pt:Ni:Cr = 28:36:36 at.%) catalysts was investigated for various potential limits of 0.9, 1.1, 1.3 and 1.4 V (vs. reference hydrogen electrode, RHE). $NaBH_4$ reduced catalysts were further reduced at 900 °C for 5 min in an argon balanced hydrogen flow stream. Improved alloying was obtained by the hydrogen reduction procedure as confirmed by X-ray diffraction results. In the PtRu/C catalyst, a decrease of irreversible Ru (hydrous) oxide formation was observed when the anodic treatment was performed at 1.1 V (vs. RHE) or higher potentials. In chronoamperometry testing performed for 60 min at 0.6 V (vs. RHE), the highest activity of the PtRu/C catalyst was observed when anodic treatment was performed at 1.3 V (vs. RHE). The current density increased from 1.71 to 4.06 A $g_{cat.}^{-1}$ after the anodic treatment. In the PtNiCr/C catalyst, dissolution of Ni and Cr was observed when potentials ≥1.3 V (vs. RHE) were applied during the anodic treatment. In MOR activity tests, the current density of the PtNiCr/C catalyst dramatically increased by more than 13.5 times (from 0.182 to 2.47 A $g_{cat.}^{-1}$) when an anodic treatment was performed at 1.4 V. On an A $g_{noble\ metal}^{-1}$ basis, the current density of PtNiCr-1.4V is slightly higher than the best anodically treated PtRu-1.3V catalyst, suggesting the PtNiCr catalyst is a promising candidate to replace the PtRu catalysts.

1. Introduction

Increasing power consumption of by portable electronics requires improved power sources with higher power density and short recharge times. Current lithium ion batteries are approaching their power density limit and require long recharge times. Direct methanol fuel cells (DMFCs) are a promising alternative to lithium ion batteries due to their high energy density and short re-fuel time. DMFCs use methanol and oxygen as the anode and cathode reactants, respectively, to produce electricity, water, and carbon dioxide. The direct use of a liquid fuel is an attractive feature of DMFCs for mobile electronic applications because of the easy handling of methanol. However, the use of methanol can also cause a decrease in the anode performance compared with pure hydrogen due to low methanol electro-oxidation reaction (MOR) activity of some anode catalysts [1]. Pt anode catalysts exhibit rapid activity loss because of easy CO poisoning, which is an intermediate of the MOR. Incorporation of Ru into the Pt catalyst can dramatically reduce the CO poisoning [2–4]. Further modification of alloy composition via transition metal incorporation can lower costs and improve MOR performance, as shown by ternary metal alloys including PtRuFe [5,6], PtRuCo [7–9], PtRuW [7], PtRuMo [10], and PtRuNi [11,12].

Optimizing improved ternary or quaternary catalyst compositions is difficult because of the many possible combinations of metals and compositions. The challenge can be lessened by employing a combinatorial approach where parallel processing and screening of compositions can be used to identify the most promising candidate compositions [13]. Sputter deposition has been used to deposit thin film libraries of candidate compounds [7,8,14–18]. In several reports it was noted that "conditioning" of the library led to enhanced activity. For example, in a Pt–Ru–Co library, all samples except $Pt_{17}Ru_{17}Co_{66}$ (at.%) showed little to no response for the MOR after deposition and annealing [7]. However, after the conditioning process, many compositions showed much larger response for the MOR with the best composition identified as $Pt_{12}Ru_{50}Co_{38}$. The conditioning process consisted of cyclic voltammetry (CV) at 60 °C for 10 cycles between −0.06 and 1.34 V (vs. reference hydrogen electrode, RHE) at a scan rate of 10 mV s^{-1}. The initially active $Pt_{17}Ru_{17}Co_{66}$ showed reduced activity after cycling, presumably due to corrosion during the conditioning process. Thin film libraries in other compositional systems (Pt–Ru–W [7] and Pt–Ni–Cr [19]) also exhibited improved MOR activity after the conditioning process. In those studies the nature of the surface modification responsible for the activity enhancement was not clear.

* Corresponding author. Tel.: +1 574 631 6151; fax: +1 574 631 8366.
E-mail address: mcginn.1@nd.edu (P.J. McGinn).

0378-7753/$ – see front matter © 2008 Elsevier B.V. All rights reserved.
doi:10.1016/j.jpowsour.2008.11.102

A recent study by Lu et al. [20] offers insight, because the anodic treatment procedure they employed is similar to the thin film library conditioning process. In that study, it was observed that anodic treatment could improve the initial MOR activity of PtRu/C powder catalysts by up to five times by a decrease of irreversible Ru (hydrous) oxides (associated with a low degree of Ru alloying) and the formation of reversible Ru (hydrous) oxides (implying a high degree of Ru alloying). They claimed that the irreversible Ru (hydrous) oxides are harmful for MOR while the reversible ones are beneficial. Additionally, in other reports it was suggested that Ru hydrous oxide is more active for the MOR than metallic Ru, with both being far more active than RuO_2 (i.e., Ru hydrous oxide > Ru metal ≫ RuO_2) [21–28]. In this study, we apply an anodic treatment to powder versions of the PtRu/C and PtNiCr/C catalyst compositions examined previously in thin film form to verify the effect of an anodic treatment on MOR activity improvement, and also to better understand how anodic treatment can improve the MOR activity of the combinatorial libraries.

2. Experimental

2.1. Catalyst preparation

The PtRu/C ("PtRu–$NaBH_4$", Pt:Ru = 50:50 at.%) and PtNiCr/C ("PtNiCr–$NaBH_4$", Pt:Ni:Cr = 28:36:36 at.%) catalysts were synthesized by a $NaBH_4$ reduction method, which was discussed in detail previously [29]. Metal precursors were dissolved in a mixture of methanol and de-ionized (DI) water. $H_2PtCl_6{\bullet}6H_2O$, $RuCl_3(H_2O$, $NiCl_2$, and $Cr(NO_3)_3(9H_2O$ were used as metal precursors of Pt, Ru, Ni, and Cr, respectively. Carbon support (Vulcan XC72R) was added to the mixture solution and then sonicated for homogeneous mixing. The mixture was stirred for 30 min and then 0.2 M $NaBH_4$ solution was added to reduce the metal precursors. The resulting mixture was further stirred for 1 h followed by filtering and washing with DI water. The resulting powder was dried in an oven at 100 °C overnight. Loading of metals was 20 wt.% of the total catalyst mass.

The $NaBH_4$ reduced catalysts were further reduced at 900 °C for 5 min under H_2/Ar flow (5.2 mol.% H_2) to ensure formation of a fully reduced metallic surface. The temperature and time for reduction was the same condition used for the combinatorial libraries previously reported [7,19]. To permit high temperature catalyst processing for such a short time, a rapid insertion technique was used to eliminate extensive ramping time. First, the catalysts were placed in a cold end of a tube furnace and H_2/Ar gas was flowed for 1 h before heating the furnace. When the furnace reached to 900 °C, the catalysts were inserted into the hot zone within 10 s via a magnetic pushing device outside the tube, and then similarly quickly extracted from the hot zone after the reduction treatment. The resulting annealed catalysts are named as "PtRu-900" and "PtNiCr-900" for the PtRu/C and PtNiCr/C catalysts, respectively. The PtNiCr-900 catalyst is the same sample discussed previously [29].

2.2. Anodic treatment and physical and electrochemical characterization

X-ray diffraction (XRD) was performed on the powder catalysts in a step scan mode with a step size of 0.02° and duration time of 0.5 s for each step from 20 to 80° 2θ.

Electrochemical characterization was performed in a beaker-type three-electrode cell. A glassy carbon electrode (3 mm dia., BAS Co., Ltd., MF-2012) was used as the working electrode. Catalyst layers were deposited by using a thin-film method [30]. The catalyst was dispersed in a mixture of DI water and Nafion ionomer solution. The mixture was sonicated to get homogeneous mixing and then a small amount of the mixture was dripped on the glassy carbon electrode. After the catalyst layer was dried in air, 5 wt.% Nafion ionomer solution was dripped on the catalyst layer to stabilize it. Platinum mesh and standard calomel electrodes were used as the counter and reference electrodes, respectively. Anodic treatment was performed by potential cycling between 0 V (vs. RHE) and the desired potentials (0.9, 1.1, 1.3, and 1.4 V vs. RHE) for 50 cycles at a scan rate of 50 mV s^{-1} at 60 °C. In the following sections of the paper, the catalysts which received anodic treatment are named by their "catalyst-potential"; for example, "PtRu-0.9V" and "PtNiCr-0.9V" are PtRu-900 and PtNiCr-900 catalysts which received anodic treatment between 0 and 0.9 V, respectively. 0.5 M H_2SO_4 solution was used as the electrolyte. For MOR activity measurement, cyclic and chronoamperometric tests were performed by potential cycling from 0 to 0.8 V at a scan rate of 50 mV s^{-1}, and by keeping the electrodes at 0.6 V (vs. RHE) for 1 h, respectively. 1 M H_2SO_4 + 1 M methanol solution was used as the electrolyte for both tests. All potentials in this paper were converted to RHE scale.

3. Results and discussion

XRD patterns of the PtRu–$NaBH_4$ and PtRu-900 catalysts are shown in Fig. 1. In the PtRu-900 catalyst, shifting and sharpening of peaks was observed, indicating changes in the degree of alloying and crystallite size, respectively. In the PtRu-900 catalyst, a new peak was observed at 43.24° from the hcp Ru (1 0 1) peak. However, the position of this peak was lower than the 44.02° value in pure Ru (ICDD PDF #65-1863), which means some Pt was incorporated into the hcp Ru phase. The Pt peaks moved to higher 2θ values after the hydrogen reduction. The Pt (1 1 1) peak at 40.03° in PtRu–$NaBH_4$ moved to 40.11° in PtRu-900, indicating a higher degree of alloying developed in the Ru-doped Pt phase. According to the equilibrium phase diagram, up to 62 at.% Ru is soluble in Pt [31]. Observation of a Ru peak after annealing indicates that some of the Ru may reduce separately from the Pt during borohydride reduction (i.e., that not all the Ru is alloyed with the Pt). The brief (5 min) thermal reduction reveals the existence of this separated Ru. Longer annealing at 900 °C would promote more complete alloying, but at the expense of severe particle coarsening. Thus, these results show that (1) some phase separation occurred after annealing of the metastable PtRu intermetallic phase resulting from borohydride reduction and (2) the separated phases are predominantly Ru-doped Pt with a minor amount of Pt-doped Ru. Crystallite sizes were calculated from the Pt (1 1 1) peaks by using the Scherrer equation [32], yielding values of 3.2 and 7.9 nm for the PtRu–$NaBH_4$ and PtRu-900 catalysts, respectively. The results for the PtNiCr–$NaBH_4$ and PtNiCr-900 were reported previously as 2.1 and 9.0 nm, respectively, with the PtNiCr-900 catalyst exhibiting a shift of peaks to higher 2θ values compared to the PtNiCr–$NaBH_4$ [29].

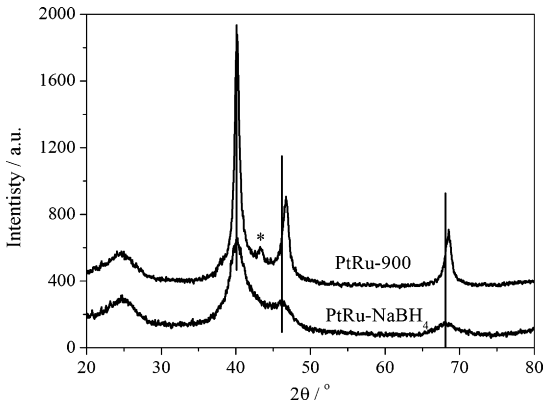

Fig. 1. XRD patterns of the PtRu–$NaBH_4$ and PtRu-900 catalysts. The (1 0 1) peak from Ru (hcp) is denoted by an asterisk.

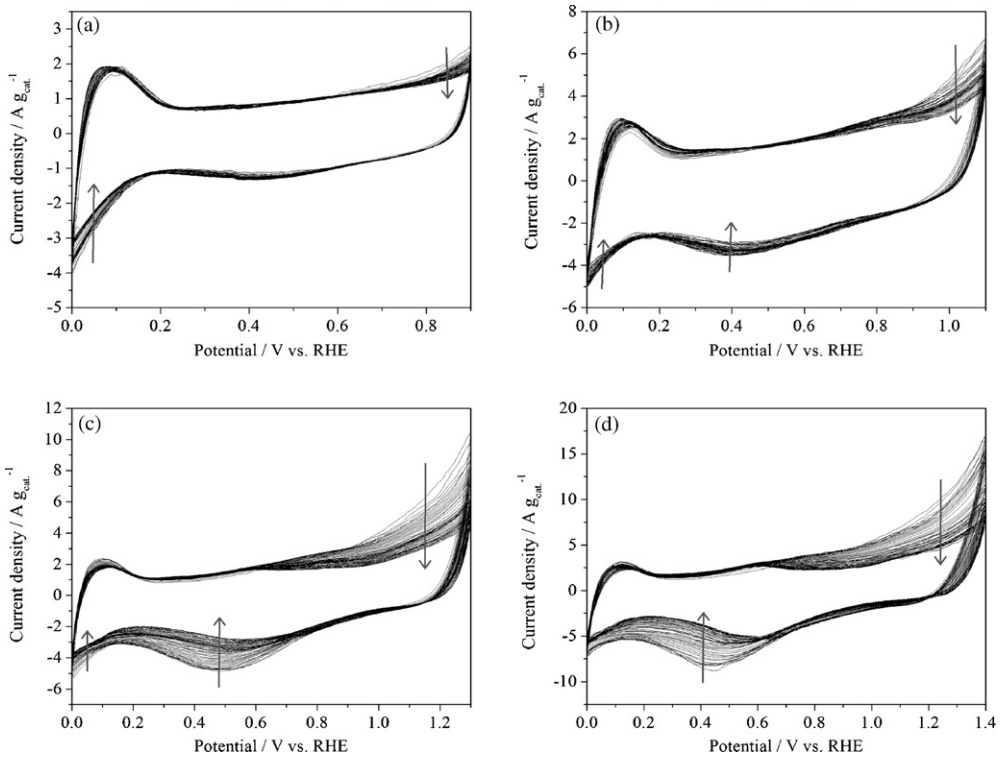

Fig. 2. Anodic treatment results of the PtRu-900 catalyst for different potential ranges between 0 and (a) 0.9, (b) 1.1, (c) 1.3, and (d) 1.4 V. Potential was cycled for 50 times at a scan rate was 50 mV s^{-1} and 60 °C. 0.5 M H_2SO_4 solution was used as the electrolyte.

Fig. 2 shows the anodic treatment results of the PtRu-900 catalyst for different potential ranges of 0.9, 1.1, 1.3, and 1.4 V. The trend change of current density with increasing number of cycles is denoted by the arrows. With increasing limiting potential, significant changes were observed above 0.7 V along the positive scan direction and between 0 and 0.6 V along the negative direction. The decrease of current density in both directions indicates a decrease of irreversible Ru (hydrous) oxide formation [20]. One point to be noted is the change of the CV curves at high potentials. Lu et al. [20] compared CV curves of high- and low-degree of alloying samples, and observed significant changes in the anodic direction of the CV curve. In samples with a high degree of alloying, a decrease of current density was observed only above 0.7 V as in the present results, while it was observed above 0.3 V in catalysts with a low degree of alloying. The change in the CV curves in this paper matches well with the sample in Lu's work with a high degree of alloying, indicating that the hydrogen reduction process produces a PtRu catalyst with a relatively high degree of alloying. One concern that should be mentioned is the possibility of Ru dissolution during the CV processing, because the decrease of the irreversible Ru (hydrous) oxides can result in the formation of reversible Ru (hydrous) oxides formation and Ru dissolution. In the results, no noticeable changes in proton desorption area (0–0.3 V along the positive scan direction) were observed, which implies no increase of Pt surface area. Thus, we can conclude that the anodic treatment caused reversible Ru (hydrous) oxide formation but not Ru dissolution.

The MOR activity measurement results for the PtRu-900 catalyst before and after anodic treatments are shown in Fig. 3(a) and (b). In Fig. 3(a), the MOR activity measured by potential cycling between 0 and 0.8 V is shown. The difference in MOR activity between PtRu-900 and PtRu-0.9V was relatively insignificant, while activity dramatically increased in PtRu-1.1V and PtRu-1.3V samples. The PtRu-1.4V catalyst did not show any further changes in the MOR activity compared to the 1.3 V treated sample. The

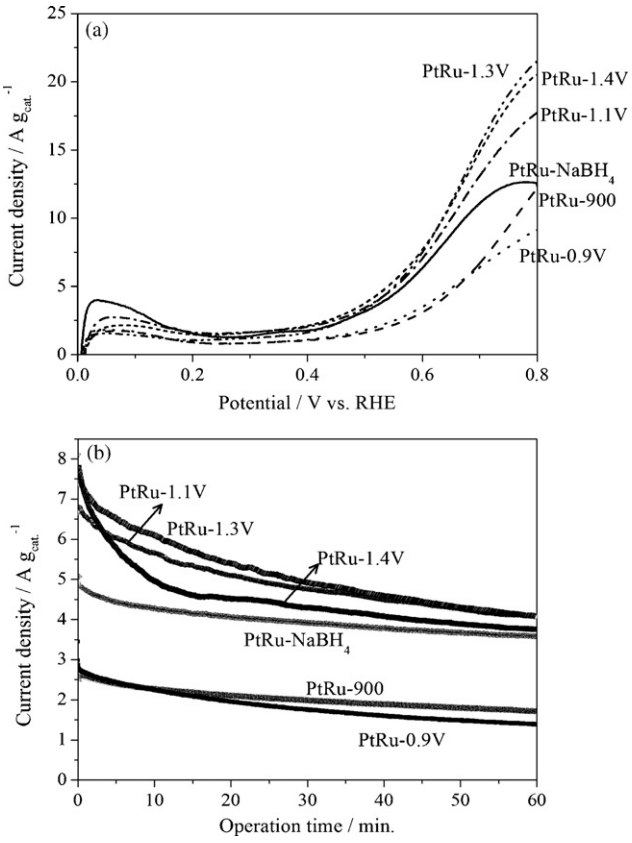

Fig. 3. MOR activity measurement results of the PtRu/C catalysts obtained by (a) potential cycling between 0 and 0.8 V at a scan rate of 50 mV s^{-1} and (b) chronoamperometry tests at 0.6 V for 60 min 1 M H_2SO_4 + 1 M methanol solution was used as the electrolyte. Both tests were performed at room temperature.

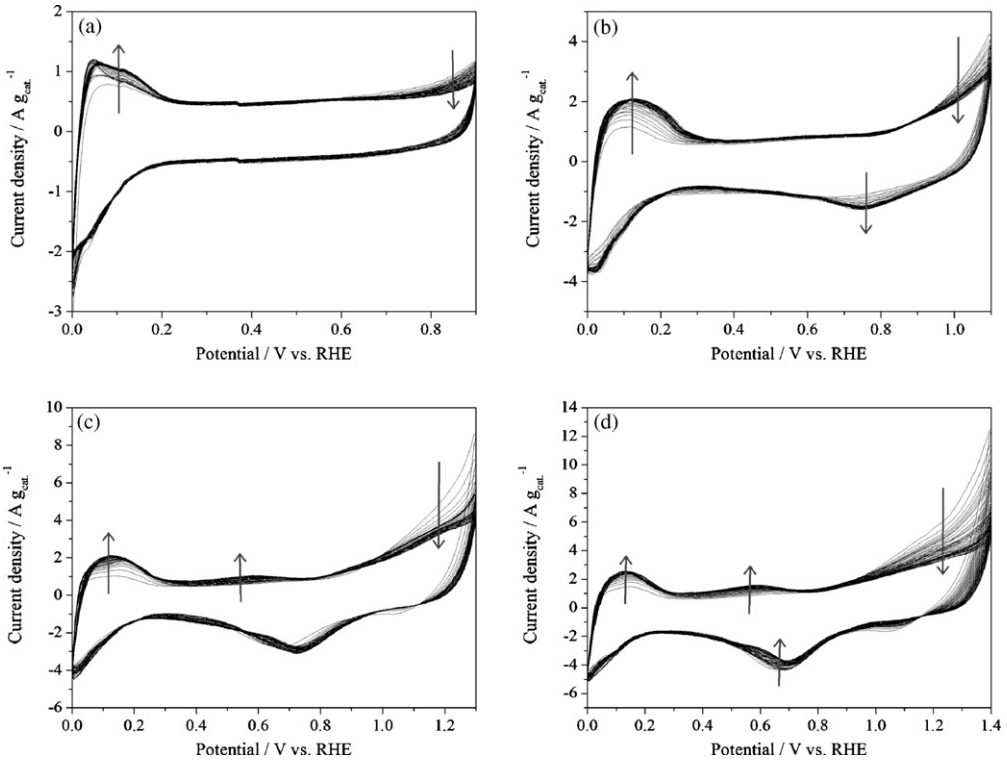

Fig. 4. Anodic treatment results of the PtNiCr-900 catalyst for different potential ranges between 0 and (a) 0.9, (b) 1.1, (c) 1.3, and (d) 1.4 V. Potential was cycled for 50 times at a scan rate was 50 mV s^{-1} and 60 °C. 0.5 M H_2SO_4 solution was used as the electrolyte.

optimum condition of 1.3 V is the same as in a previous report where a commercial catalyst was used [20], which contained a large amount of Ru (hydrous) oxides [21]. In chronoamperometry tests, Fig. 3(b), the PtRu-1.1V and PtRu-1.3V catalysts showed the same current density of 4.06 A $g_{cat.}^{-1}$ at 60 min, which were even higher than the 3.58 A $g_{cat.}^{-1}$ value of the as-reduced PtRu–$NaBH_4$ catalyst. Considering the much larger crystallite size of the PtRu-1.1V and PtRu-1.3V catalysts, this increase of current density shows the importance of the surface Ru oxidation state. When compared with the 1.71 A $g_{cat.}^{-1}$ value for the PtRu-900 catalyst, the current density of the PtRu-1.1V and PtRu-1.3V catalysts is 137% higher. This result confirms that, for high MOR activity, the Ru (hydrous) oxides are more beneficial than metallic Ru, as was suggested in recent publications [20–28].

Fig. 4 shows the anodic treatment results for the PtNiCr-900 catalyst. The PtNiCr catalysts showed a decrease of current density above 0.9 V along the positive scan direction, like the PtRu case. However, we observed a small decrease of current density at 0.65 V along the negative scan direction, which means that the decrease of current density came from dissolution of Ni and Cr. Also the noticeable increase in the current density of the proton desorption area shows that dissolution of Ni and Cr caused exposure of Pt on the catalyst surface. A difference of the PtNiCr/C catalysts from the PtRu/C catalysts is that no changes were observed along the negative scan direction. In the PtRu/C catalysts, a decrease of current density in 0–0.6 V along the negative scan direction was observed that was caused by a decrease in irreversible Ru (hydrous) oxide formation. The absence of changes along the negative scan direction means that both the dissolution of Ni and Cr (which leads to a current density increase from more Pt surface exposure) and a decrease of irreversible Ni and Cr (hydrous) oxides (which cause current density decrease) were induced by the anodic treatments. The cause for the increase of current density observed near 0.5 V in PtNiCr-1.3V and PtNiCr-1.4V catalysts is not presently understood. One possible explanation is oxidation of reversible or partially reduced Ni and Cr (hydrous) oxides, but more detailed research is required to verify the mechanism.

Fig. 5 shows the MOR activity measurement results of the PtNiCr catalysts. The PtNiCr-900 and PtNiCr-0.9V catalysts showed no significant differences, similar to the PtRu catalysts, but with increasing limiting potential an increase of current density was observed. One difference from the PtRu case is the PtNiCr-1.4V catalyst, which exhibited the highest MOR activity, in contrast to PtRu where there were no changes between the PtRu-1.3V and PtRu-1.4V catalysts. This indicates that a different anodic treatment condition is needed for different alloys to produce the optimum metal (hydrous) oxide state. In chronoamperometry tests shown in Fig. 5(b), the improvement in MOR activity resulting from higher anodic treatment potential was clearly shown. The order of activities was not changed during the chronoamperometry tests. However, much higher current density was observed in the PtNiCr-0.9V catalyst than in the PtNiCr-900 catalyst, which might come from the increased number of exposed Pt atoms on the catalyst surface due to slight dissolution of Ni and Cr as mentioned in the CV results. The current density in the PtNiCr-1.4V was 2.47 A $g_{cat.}^{-1}$ which is more than 1260% higher than 0.182 A $g_{cat.}^{-1}$ in the PtNiCr-900 catalyst (not anodically treated). This dramatic change in the PtNiCr catalyst may result from Pt and/or NiCr (hydrous) oxide contributions. Based on the CV results, it is clear that both a Pt surface increase and oxidation of NiCr occur simultaneously. The Pt surface area did not increase enough to account for all of the performance improvement, so Ni and Cr must also significantly contribute to the increased MOR activity in their reversible (hydrous) oxide forms. Also this result implies that the effect of anodic treatment between metallic and reversible (hydrous) oxide forms is much greater in the PtNiCr system than in the PtRu system. The curve for PtRu–$NaBH_4$ from Fig. 3b is also shown in Fig. 5b for comparison. It shows that the best anodically treated PtNiCr powder is still outperformed by the non-anodically treated PtRu. However, on an A $g_{noble\ metal}^{-1}$ basis, current density

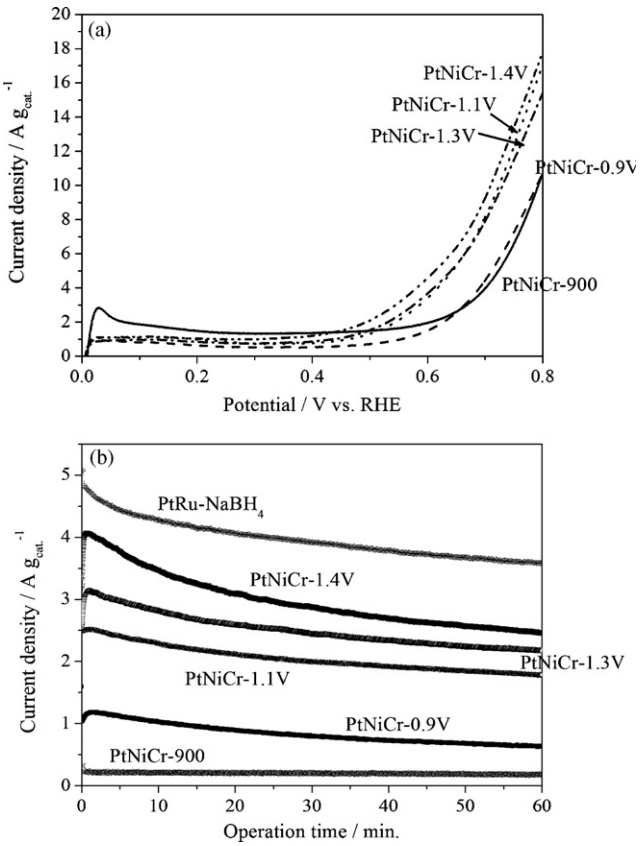

Fig. 5. MOR activity measurement results of the PtNiCr/C catalysts obtained by (a) potential cycling between 0 and 0.8 V at a scan rate of 50 mV s^{-1} and (b) chronoamperometry tests at 0.6 V for 60 min 1 M H_2SO_4 + 1 M methanol solution was used as the electrolyte. Both tests were performed at room temperature.

of PtNiCr-1.4V is 21.4 A $g_{noble\ metal}^{-1}$ which is 20% higher than 17.9 A $g_{noble\ metal}^{-1}$ in the PtRu–$NaBH_4$ catalyst. The activity of the PtNiCr-1.4V is even slightly higher than the best anodically treated PtRu-1.3V catalyst which exhibited 20.3 A $g_{noble\ metal}^{-1}$, suggesting the PtNiCr catalyst is a promising candidate to replace the PtRu catalysts.

The results of this paper on the anodic treatment provide an important clue to understand the conditioning process which we reported in a previous study on thin film combinatorial Pt–Ru–W and Pt–Ru–Co libraries [7]. The anodic treatment results in this paper clarify the improved MOR activity of the libraries after the conditioning tests via the formation of reversible (hydrous) oxides. Though the initial conditioning process applied to the thin film libraries was not based on the expectation of the anodic treatment effect, these results show that a conditioning process can make the libraries closer in behavior to well-optimized and powder-like forms. However, in the powder study, the increase of MOR activity was less than in the library results, which might be due to the (111) preferred orientation of the thin film libraries [4,33] and possibly different surface compositions between the libraries and powder form catalysts. As discussed in previous reports [7,8], optimum compositions of the PtRu catalyst in thin film and powders are quite different. In thin films, 10–20 at.% of Ru exhibits the best MOR performance [4,7,33,34], while 50 at.% of Ru is the best composition in powder catalysts [35,36]. Hence, there is not always a direct correlation between the results in thin film and powder catalysts. But, the results shown in this paper suggest that an anodic treatment is an important component of a thin film screening protocol, to improve the correlation between thin film and bulk powder performance.

4. Conclusion

The effect of anodic treatment on the PtRu/C and PtNiCr/C catalysts was investigated. By choosing the optimum potentials for anodic treatment, both of the catalysts showed dramatic increase of MOR activity. The MOR activity of PtRu-900 catalyst (chronoamperometry at 60 min) increased from 1.71 to 4.06 A $g_{cat.}^{-1}$ in the PtRu-1.3 V catalyst, which is a 137% increase of current density. For the PtNiCr-900 catalyst, the MOR activity increased from 0.182 to 2.47 A $g_{cat.}^{-1}$ in the PtNiCr-1.4V catalyst, which is a 1260% increase of current density. These results prove that the reversible (hydrous) oxide forms of Ru, Ni, and Cr is more beneficial than their metallic forms to improve the MOR activity. Also, an anodic conditioning process is a useful way to form reversible (hydrous) oxides, and should be included as a component of combinatorial screening of thin film libraries to reduce possible differences between the well-reduced surface thin film libraries and low temperature synthesized powder forms of catalysts.

Acknowledgements

This work was partially supported by the U.S. Army CECOM RDEC through Agreement DAAB07-03-3-K414 and by the Department of Defense and the Army Research Office through contract numbers W911QX06C0117 and W911NF08C0037. Such support does not constitute endorsement by the U.S. Army of the views expressed in this publication.

References

[1] A.S. Arico, S. Srinivasan, V. Antonucci, Fuel Cells 1 (2001) 133–161.
[2] M. Watanabe, S. Motoo, J. Electroanal. Chem. 60 (1975) 267–273.
[3] N.M. Markovic, H.A. Gasteiger, P.N. Ross Jr., Electrochim. Acta 40 (1995) 91–98.
[4] W. Chrzanowski, A. Wieckowski, Langmuir 14 (1998) 1967–1970.
[5] M.K. Jeon, J.Y. Won, K.R. Lee, S.I. Woo, Electrochem. Commun. 9 (2007) 2163–2166.
[6] M.K. Jeon, K.R. Lee, H. Daimon, A. Nakahara, S.I. Woo, Catal. Today 132 (2008) 123–126.
[7] J.S. Cooper, P.J. McGinn, J. Power Sources 163 (2006) 330–338.
[8] P. Strasser, J. Comb. Chem. 10 (2008) 216–224.
[9] S. Pasupathi, V. Tricoli, J. Solid State Electrochem. 12 (2008) 1093–1100.
[10] A. Oliveira Neto, E.G. Franco, E. Arico, M. Linardi, E.R. Gonzalez, J. Eur. Ceram. Soc. 23 (2003) 2987–2992.
[11] J. Liu, J. Cao, Q. Huang, X. Li, Z. Zou, H. Yang, J. Power Sources 175 (2008) 159–165.
[12] J.H. Choi, K.W. Park, B.K. Kwon, Y.E. Sung, J. Electrochem. Soc. 150 (2003) A973–A978.
[13] E. Reddington, A. Sapienza, B. Gurau, R. Viswanathan, S. Sarangapani, E.S. Smotkin, T.E. Mallouk, Science 280 (1998) 1735–1737.
[14] S. Guerin, B.E. Hayden, C.E. Lee, C. Mormiche, J.R. Owen, A.E. Russell, J. Comb. Chem. 6 (2004) 149–158.
[15] P. Strasser, Q. Fan, M. Devenney, W.H. Weinberg, P. Liu, J.K. Nørskov, J. Phys. Chem. B 107 (2003) 11013–11021.
[16] J.S. Cooper, G. Zhang, P.J. McGinn, Rev. Sci. Instrum. 76 (2005) 062221.
[17] T. He, E. Kreidler, Phys. Chem. Chem. Phys. 10 (2008) 3731–3738.
[18] M.D. Fleischauer, T.D. Hatchard, G.P. Rockwell, J.M. Topple, S. Trussler, S.K. Jericho, M.H. Jericho, J.R. Dahn, J. Electrochem. Soc. 150 (2003) A1465–A1469.
[19] J.S. Cooper, M.K. Jeon, P.J. McGinn, Electrochem. Commun. 10 (2008) 1545–1547.
[20] Q. Lu, B. Yang, L. Zhuang, J. Lu, J. Phys. Chem. B 109 (2005) 1715–1722.
[21] D.R. Rolison, P.L. Hagans, K.E. Swider, J.W. Long, Langmuir 15 (1999) 774–779.
[22] J.W. Long, R.M. Stroud, K.E. Swider-Lyons, D.R. Rolison, J. Phys. Chem. B 104 (2000) 9772–9776.
[23] M.K. Jeon, J.Y. Won, S.I. Woo, Electrochem. Solid-state Lett. 10 (2007) B23–B25.
[24] A.N. Gavrilov, E.R. Savinova, P.A. Simonov, V.I. Zaikovskii, S.V. Cherepanova, G.A. Tsirlina, V.N. Parmon, Phys. Chem. Chem. Phys. 9 (2007) 5476–5489.
[25] K. Lasch, L. Jörissen, K.A. Friedrich, J. Garche, J. Solid State Electrochem. 7 (2003) 619–625.
[26] O.A. Petrii, J. Solid State Electrochem. 12 (2008) 609–642.
[27] A. Rose, E.M. Crabb, Y. Qian, M.K. Ravikumar, P.P. Wells, R.J.K. Wiltshire, J. Yao, R. Bilsborrow, F. Mosselmans, A.E. Russell, Electrochim. Acta 52 (2007) 5556–5564.
[28] J.S. Spendelow, P.K. Babu, A. Wieckowski, Curr. Opin. Solid State Mater. Sci. 9 (2005) 37–48.
[29] M.K. Jeon, Y. Zhang, P.J. McGinn, Electrochim. Acta, in press, doi:10.1016/j.electacta.2008.11.027.
[30] T.J. Schmidt, H.A. Gasteiger, G.D. Stäb, P.M. Urban, D.M. Kolb, R.J. Behm, J. Electrochem. Soc. 145 (1998) 2354–2358.

[31] T.B. Massalski, H. Okamoto, P.R. Subramanian, L. Kacprzak, Binary Alloy Phase Diagrams, 2nd ed., ASM International, OH, USA, 1990.
[32] C.Z. He, H.R. Kunz, J.M. Fenton, J. Electrochem. Soc. 144 (1997) 970–979.
[33] H.A. Gasteiger, N. Markovic, P.N. Ross Jr., E.J. Cairns, J. Phys. Chem. 97 (1993) 12020–12029.
[34] J.F. Whitacre, T. Valdez, S.R. Narayanan, J. Electrochem. Soc. 152 (2005) A1780–A1789.
[35] J.B. Goodenough, R. Manoharan, Chem. Mater. 1 (1989) 391–398.
[36] A.J. Dickinson, L.P.L. Carrette, J.A. Collins, K.A. Friedrich, U. Stimming, J. Appl. Electrochem. 34 (2004) 975–980.